Optimal Features Extraction of Noisy Sinusoidal Signals Using Two-Stage Linear Least Squares Fitting *

Huifang Dou and YangQuan Chen
Mechatronics and Automation Laboratory
Department of Electrical Engineering
National University of Singapore
10 Kent Ridge Crescent, Singapore 119260
Email: yqchen@ieee.org

Abstract

Abstract This technical memo documents two small but practically useful MATLAB scripts for optimal extraction of features in sampled noisy sinusoidal signals. They are useful in automatic measurement of amplitude, frequency as well as phase shift of a sampled noisy sinusoidal signal series. Detailed descriptions and user's guide are given with several application examples.
Key Words: Feature extraction, least squares, optimization.

1 Introduction

In many applications, it is required to measure the amplitude, frequency and also phase shift quantities from sampled noisy sinusoidal signal series. Some times, the frequency is exactly known while in some cases, the frequency is only approximately known. For example, in relay autotuning experiments, the selfinduced controlled oscillations can be recorded via data sampling through an AD/DA card. The amplitude and the frequency are two important parameters for the PI/PID controller tuning task.

This is actually an easy task using least squares (LS) fitting. However, when three features, i.e., frequency, amplitude and phase shift are to be extracted, a nonlinear LS method has to be applied. In this work, a simplified yet practical idea is used. First, the frequency is fixed. Then, the LS can be converted into a linear one. The remaining problem is a one dimensional optimization with respect to the frequency which can be done efficiently using '`fmin`' provided in MATLAB.

*The authors are now with the Center for Self-Organizing and Intelligent Systems (CSOIS), Dept. of Electrical and Computer Engineering, Utah State University, 4160 Old Main Hill, Logan, Utah 84322-4160. Tel: (435)7970148, Fax: (435)7973054, email: {yqchen,douhf}@ece.usu.edu. Url: http://www.csois.usu.edu/people/yqchen/. First draft: Oct. 1998.

2 Numerical Methods

Denote $\{\bar{y}(t) \mid t = t_0, t_0 + T_s, \cdots, t_0 + (N_p - 1)T_s\}$ a data series of a sampled noisy sinusoidal signal where N_p is the total number of point, T_s the sampling period in second and t_0 is the initial time in second. The true signal is

$$y(t) = A\sin(\omega t + \theta). \tag{1}$$

The optimization problem is to

$$\min_{A,\omega,\theta} J(A,\omega,\theta) = \sum_{j=0}^{N_p-1} [\bar{y}(t_0 + jT_s) - y(t_0 + jT_s)]^2 \tag{2}$$

This is clearly a nonlinear least squares problem. As shown in what follows, this can be simplified to a two stage linear least squares problems.

2.1 Fixed ω

When ω is fixed, (2) can be converted to a linear LS problem. By taking

$$\alpha_1 = A\sin(\theta), \quad , \alpha_2 = A\cos(\theta), \tag{3}$$

for a given ω, the optimization problem is to

$$\min_{A,\theta} J_\omega(A,\theta) = \sum_{j=0}^{N_p-1} [\bar{y}(t_0 + jT_s) - \alpha_1 \sin(\omega(t_0 + jT_s)) - \alpha_2 \cos(\omega(t_0 + jT_s))]^2 \tag{4}$$

which is clearly a linear LS problem and can be easily solved.

2.2 Optimizing ω

Obviously, it can be defined that

$$\min_{A,\omega,\theta} J(A,\omega,\theta) = \min_{\omega}\{\min_{A,\theta} J_\omega(A,\theta)\} \tag{5}$$

which can be done efficiently using '`fmin`' provided in **MATLAB**.

3 Examples

3.1 Better Estimation of Ultimate Amplitude and Frequency for Relay Test

A relay tuning response is shown in Fig. 1 where $T_s = 0.001$ sec. A rough estimate of the frequency can be obtained as 10/3 (10 cycles in 3000 points). Therefore, using the last 3000 points for the feature extraction, by calling

```
[Ahat,Theta,Omega,RMS]=sinefit(p3',3/10,2,0.001);
```

gives Fig. 2 where optimal features are displayed. Note that the calling format as shown in Appendix A.

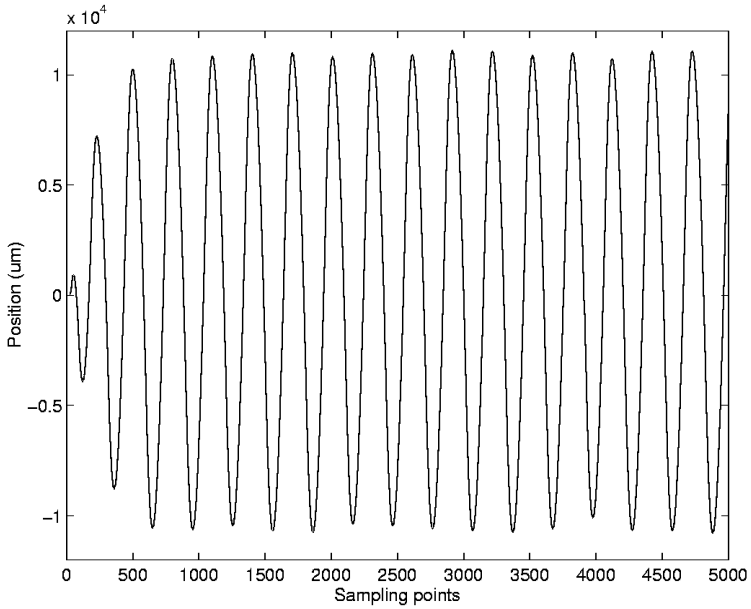

Figure 1: Positional response of a linear motor under relay test

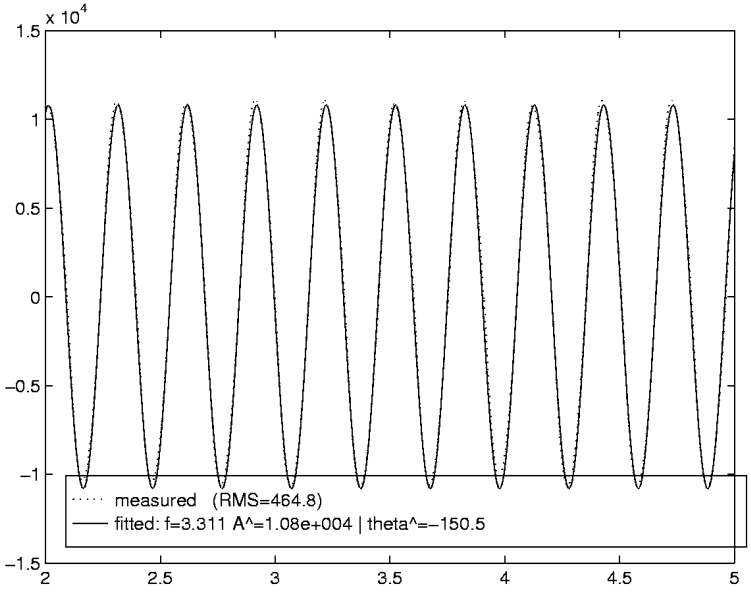

Figure 2: Feature extraction of the signal from relay test (last 3000 points)

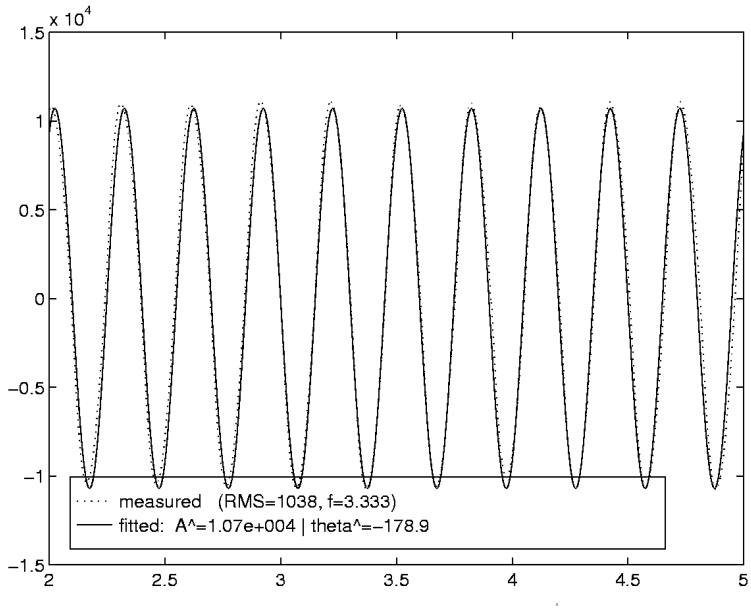

Figure 3: Feature extraction of the signal from relay test (last 3000 points, ω fixed at $2\pi * (10/3)$

When ω is fixed at the rough estimate $2\pi * (10/3)$ rad/sec., by calling
`[Ahat,Theta,RMS]=sinefit2(p3',2*pi/(3/10),2,0.001);`
gives Fig. 3 where optimal features are displayed. The calling format is selfexplained in AppendixB. Attention should be paid to the the second calling parameter. For `sinefit2`, it is ω in rad/sec. while in `sinefit`, it should be the estimated period in second.

It should be observed that the RMS in this case is 1038 which is doubly larger than that of Fig. 2. Therefore, in practice, we should use `sinefit` instead of `sinefit2` to obtain an optimal feature estimate.

3.2 Application in friction modelling and system parameter estimation through relay-tuning

Consider the process:

$$G_p(s) = \frac{10}{s(0.2685s + 1)}, \tag{6}$$

with $f_1 = 0.5, f_2 = 0.01$.

The Simulink model of the proposed dual relay tuning is shown in Fig. 4

In the simulations, $h_{1,1} = 2$, $h_{2,1} = 1.5$, $h_{1,2} = 2.5$, $h_{2,2} = 2$, and $h_{1,3} = 1$, $h_{2,3} = 0.5$ are chosen for the relay amplitudes. The limit cycle oscillations corresponding to the three experiments are shown in Figs. 5, 6 and 7. T_p and K_p are correctly identified as $T_p = 0.2446$ and $K_p = 9.1536$ respectively. At the same time, f_1 and f_2 are identified as $f_1 = 0.5402$ and $f_2 = 0.01879$ while $c_{1,2} = 1.0127$, $c_{1,3} = 0.9268$

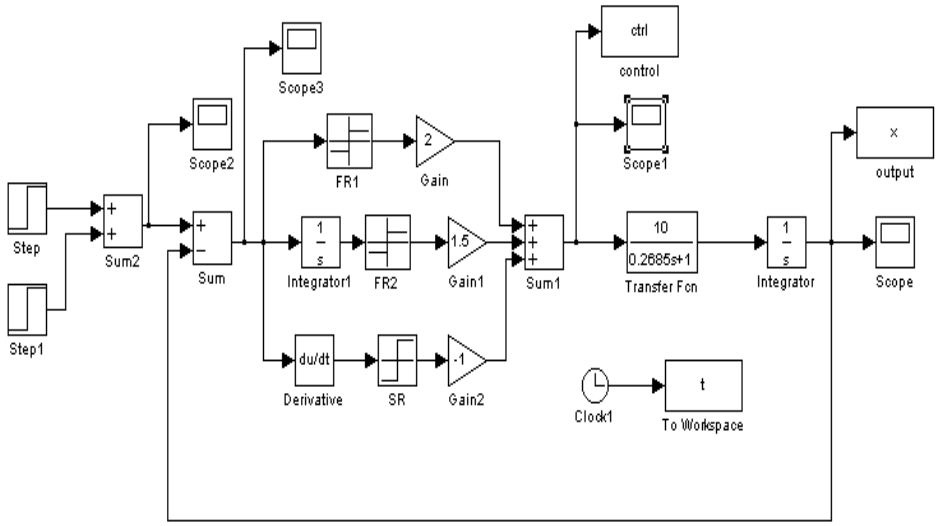

Figure 4: The Simulink model of the proposed dual relay tuning

The input and output signals with $h_{1,1} = 2$, $h_{2,1} = 1.5$ are shown in Fig. 8. By calling `[Ahat,Theta,Omega,RMS]=sinefit(s1,20/10,10,0.001);` . The optimal fitting result is given in the Fig. 9.

The system parameters are calculated through the following MMATLAB codes.

```
%Calculation of the system parameters
load para.mat
a1=1.2627 ;
a2=6.286;
a3=5.7935;
T1=4/5.5;
w1=2*pi/T1;
T2=6/5.85;
w2=2*pi/T2;
T3=10/9;
w3=2*pi/T3;
h11=2;
h21=1.5;
h12=5;
h22=4;
h13=4;
h23=3.5;
f1=(a2*(w2-w1)*(a3*w3*h21-a1*w1*h23)-a3*(w3-w1)*(a2*w2*h21-a1*w1*h22))...
/(a3*(w3-w1)*(a1*w1-a2*w2)-a2*(w2-w1)*(a1*w1-a3*w3));
f2=4*((a1*w1-a2*w2)*f1-a1*w1*h22+a2*w2*h21)/((pi*a1*a2)*(w2-w1));
%f21=4*((a1*w1-a3*w3)*f1-a1*w1*h23+a3*w3*h21)/((pi*a1*a3)*(w3-w1));
```

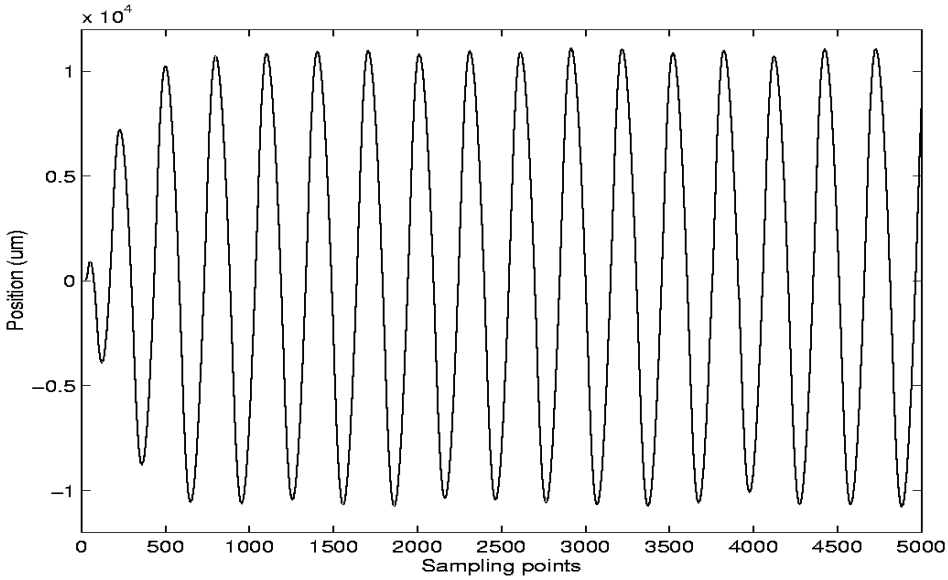

Figure 5: Relay test experiment #1

```
Kp=-pi*a1*w1/(4*(f1-h21)+pi*a1*f2);
Tp=4*h11*Kp/(pi*a1*w1*w1);
%Kp1=-pi*a2*w2/(4*(f1-h22)+pi*a2*f2);
c1=(h11*a2*w2*w2)/(h12*a1*w1*w1);
c2=(h11*a3*w3*w3)/(h13*a1*w1*w1);
```

3.3 Noise Filtering

A testing sinusoidal signal is generated by the following MATLAB codes which is corrupted with noises of normal distribution.

```
% test codes:
A0=2;sigma=1;
omega=2*pi*2; % f=2 Hz
theta0=pi/2;
t=0:.005:2;
dn=sigma*randn(size(t));
s0=A0*sin(omega*t + theta0) + dn;
t0=0;Ts=0.005;
```

Assume frequency $f = 2.5$ Hz which is 25% larger than the theoretical value of 2 Hz. Calling
`[Ahat,Theta,Omega,RMS]=sinefit(s0,0.4,0,0.005)`
gives the filtering results shown in Fig. 10. Now, increase sigma from 1 to 2. The filtering results are shown in Fig. 11 by calling
`[Ahat,Theta,Omega,RMS]=sinefit(s0,1/1.5,0,0.005)`.
Note that in this case, the frequency $f = 1.5$ Hz which is 25% lower than the theoretical

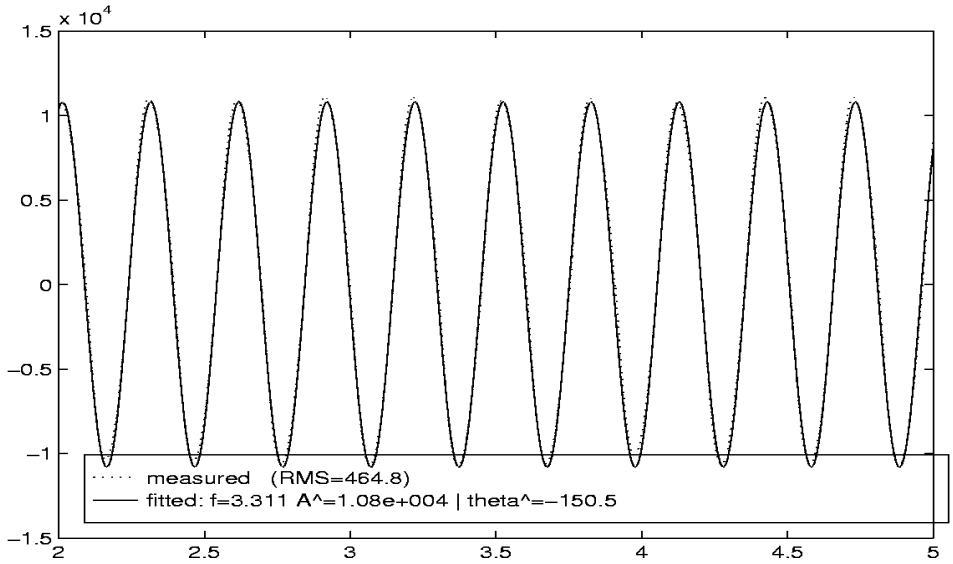

Figure 6: Relay test experiment #2

value of 2 Hz. It can be concluded that the optimal feature extraction can be used as a means of filtering.

4 Conclusion

The MATLAB scripts documented in this memo are practically useful.

A Script sinefit.m listing

```
% sine wave fitting from noisy sinusoidal signal
% phase fitting has to be considered as well as frequency
% Last modified 05-11-2000
% s0: sampled series. 1xNp
% Testim: estimated period (sec.) (may not be accurate)
% Ts: sampling period (in Sec.)
% t0: initial time (in Sec.)
% Ahat: estimated amplitude
% Theta: fitted theta_0 (in rad.)
% Omega: 2pi*freq
% RMS: root mean squares.
%
% See also: sinefit2
function [Ahat,Theta,Omega,RMS]=sinefit(s0,Testim,t0,Ts)
%
Omega=fmin('jomega',(2*pi/Testim)*.5,...
```

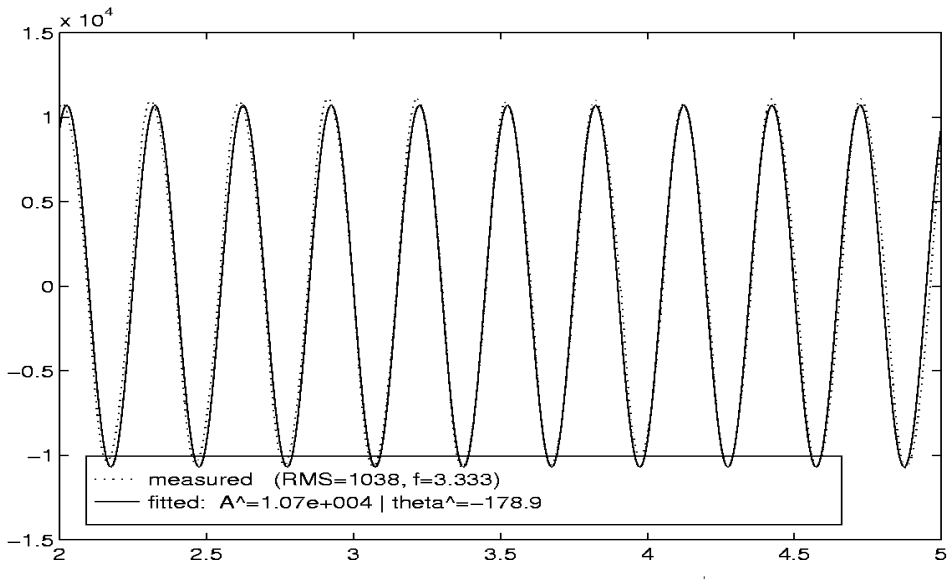

Figure 7: Relay test experiment #3

```
(2*pi/Testim)*2.0, [0,1.0e-30 ], s0,t0,Ts)
[Ahat,Theta,RMS]=sinefit2(s0,Omega,t0,Ts);

disp(['f=',num2str(Omega/2/pi),...
' | RMS=',num2str(RMS),' A ^ =', num2str(Ahat),...
' | Theta ^ =',num2str(Theta*180/pi)])
Np=size(s0);
t=t0+[0:Np(2)-1]*Ts;
figure;
plot(t,s0,'k:',t, Ahat*sin(Omega*t+Theta),'-r');
legend(['measured (RMS=',num2str(RMS),')'],...
['fitted: f=',num2str(Omega/2/pi),...
' A.hat =',num2str(Ahat),...
' |  theta.hat =',num2str(Theta*180/pi)])
return
```

B Script sinefit2.m listing

```
% sine wave fitting from noisy sine signal
% phase fitting has to be considered
% with a fixed omega!
% Last modified in 05-11-2000
% DESCRIPTIONS:
% s0: sampled series. 1xNp (note here)
% omega: known freq. (2*pi*f) (rad/sec.)
```

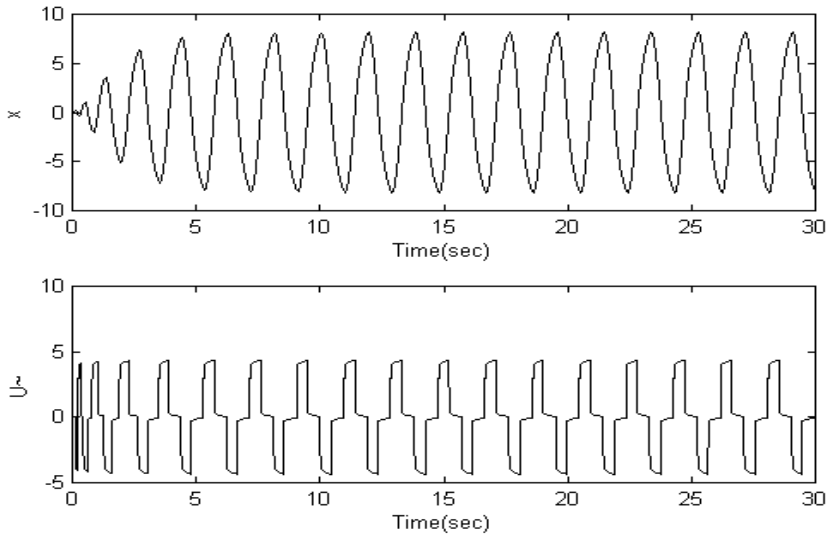

Figure 8: The input and output signals of the proposed dual relay test

```
% Ts: sampling period (in Sec.)
% t0: initial time (in Sec.)
% Ahat: estimated amplitude
% Theta: fitted theta_0 (in rad.)
% RMS: root mean squares.
%
% See also "jomega"
function [Ahat,Theta,RMS]=sinefit2(s0,omega,t0,Ts)
Np=size(s0);
t=t0+[0:Np(2)-1]*Ts;
A11= (sin(omega*t)*(sin(omega*t))');
A12= (sin(omega*t)*(cos(omega*t))');
A22= (cos(omega*t)*(cos(omega*t))');
b1=s0*(sin(omega*t))';
b2=s0*(cos(omega*t))';
A=[A11,A12;A12,A22];
Alpha=inv(A)*[b1,b2]';
% be careful here...
Asintheta=Alpha(2);Acostheta=Alpha(1);
Ahat=sqrt(Asintheta*Asintheta+Acostheta*Acostheta);
Theta=atan2(Asintheta,Acostheta);
RMS=sqrt((s0-Ahat*sin(omega*t+Theta))*...
(s0-Ahat*sin(omega*t+Theta))'/(Np(2)-1.));
if (0)
figure;
plot(t,s0,'k:',t, Ahat*sin(omega*t+Theta),'-r');
```

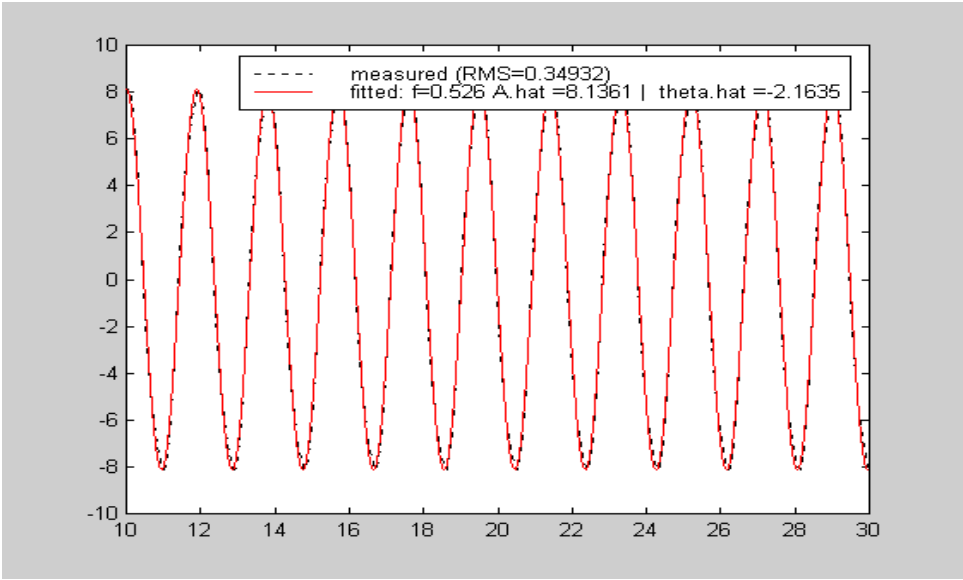

Figure 9: The optimal fitting result

```
legend(['measured (RMS=',num2str(RMS),', f=',...
num2str(omega/2/pi),')'],['fitted: ',...
' A.hat=',num2str(Ahat),' | theta.hat=',num2str(Theta*180/pi)])
end
return;
```

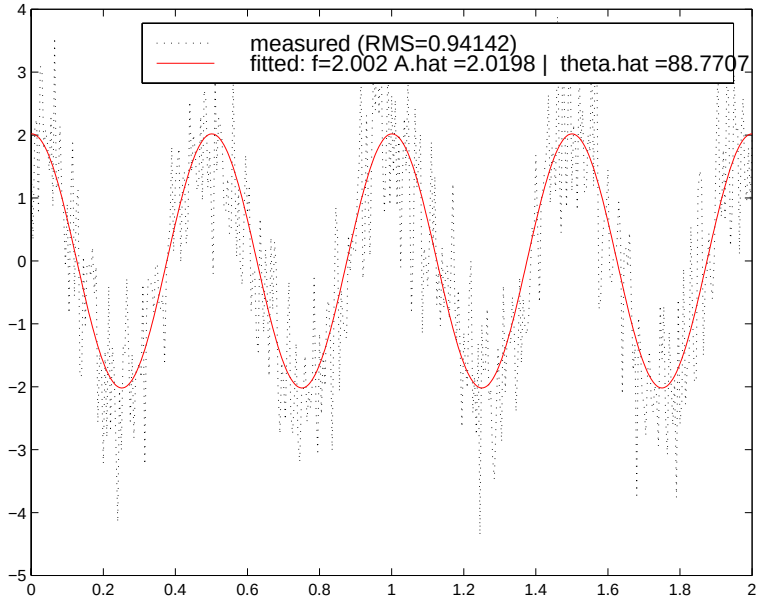

Figure 10: Feature extraction as a means of filtering (sigma=1)

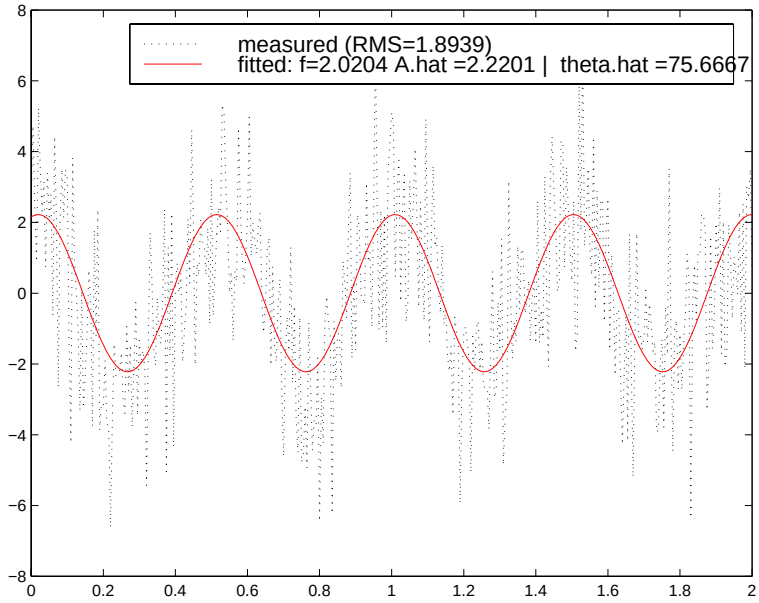

Figure 11: Feature extraction as a means of filtering (sigma=2)

Friction Modeling and Adaptive Compensation Using a Relay Feedback Approach

Department of Electrical Engineering
National University of Singapore

Abstract

In this paper, the application of a dual relay feedback approach towards modeling of frictional effects in servo-mechanisms is addressed. The friction model consists of Coulomb and viscous friction components, both of which can be automatically extracted from suitably designed relay experiments. At the same time, the dynamical model of the servo-mechanical system can be obtained from the experiments. Thus, a PID feedback motion controller and a feedforward friction compensator can be automatically tuned in this manner. The friction model obtained is also directly applicable to initialisation of an adaptive control scheme proposed. Results from simulation and experiments are presented to illustrate the practical appeal of the proposed method.

1 Introduction

The application of relay feedback to automatic tuning of controllers has been widely explored during the last decade [1]. Today, many industrial controllers are equipped with relay automatic tuning features, in one form or another. In these applications, a relay feedback apparatus is used to excite a sustained oscillation, from which information of the system can be inferred and used to tune the controller. The application domain of relay automatic tuning has been expanded since its inauguration, and today, the technology is applicable to many industrial processes [1] and servomechanisms [2]. However, thus far, the system models (implicit or explicit) derived from the relay experiments for tuning purposes are mainly linear ones. For nonlinear systems, a gain scheduling approach using multiple relay experiments at different setpoints has been largely proposed [3].

In this paper, we explore a new application of relay feedback in the identification of a friction model for servo-mechanisms. The frictional characteristics associated with servo-mechanisms are highly nonlinear in nature, and a good friction model is especially important for applications involving high precision motion control of servomechanisms, where the frictional force needs to be adequately compensated in order to improve the transient performance and to reduce steady state tracking errors. Even in adaptive control of servo-mechanisms, as will be illustrated in the paper, an initial friction model is also crucial to ensure smooth control signals and rapid parameter convergence [4]. Friction modeling has always been a difficult and challenging problem [5]-[7]. Models of varying complexity have been used to approximate the dynamics of friction [5]. However, in practical applications, models of the Tustin type are usually used which yield good consistent results in many

cases without undue structural complexity.

In [8], the idea of using relay feedback to identify a simple Coulomb friction model is first mooted. Either an iterative procedure or a noise-sensitive analysis of the limit cycles of a servo-mechanical system under relay feedback can be invoked to yield an approximation of the Coulomb friction coefficient. In this paper, we will attempt to identify key friction characteristics, including both Coulomb and viscous types, of a servo-mechanical system using only the amplitude and frequency of the limit cycle oscillations induced from relay feedback. Under a relay feedback configuration, the overall nonlinear system (with friction) can be posed as a feedback configuration comprising of an equivalent parallel relay construct acting on a linear system in the usual manner. Using this representation, friction modeling is equivalent to the identification of friction-associated characteristics using the describing function approximation. From the relay experiment, apart from the friction phenomenon, low-order dynamical characteristics of the system can also be derived. Thus, in this manner, both a feedback PID controller and a feedforward friction compensator (to further enhance tracking performance) can be automatically tuned. Since it is well-known that the friction characteristics can be time varying, an adaptive control technique is further proposed and developed to adaptively modify the initial friction model according to prevailing error signals. A stability analysis of the adaptive scheme is provided in the paper. Both simulation and a real-time experiment on a permanent magnet linear motor (PMLM) will be used to illustrate the principle and application appeal of the proposed method.

2 Model of Servo-Mechanical Systems

The dynamics of a servo-mechanical system can be described using a nonlinear mathematical model:

$$u(t) = K_e\dot{x} + Ri(t) + Ldi(t)/dt, \tag{1}$$

$$f(t) = K_f i(t), \tag{2}$$

$$f(t) = m\ddot{x}(t) + \bar{f}_{fric}(\dot{x}) + \bar{f}_{load}(t) + \bar{f}_{res}(t), \tag{3}$$

where $u(t)$ and $i(t)$ are the time-varying motor terminal voltage and armature current respectively; $x(t)$ is the motor position; $f(t)$ and $\bar{f}_{load}$ are the developed force and the applied load force respectively. $\bar{f}_{fric}$ denotes the frictional force and $\bar{f}_{res}$ represents any remaining small and uncertain unaccounted dynamics. The physical significance of the other physical parameters are highlighted (and given specific values for the Anorad LS-B series of linear motors) in Table 1 [10].

Since the electrical time constant is much smaller than the mechanical one, the transient delay due to the electrical response can be ignored. With this simplification, the following equation can be obtained [9]:

$$\ddot{x} = (-\frac{K_f K_e}{R}\dot{x} + \frac{K_f}{R}u(t) - \bar{f}_{fric} - \bar{f}_{load} - \bar{f}_{res})/m. \tag{4}$$

Let

$$a = -K_e, \tag{5}$$

$$b = \frac{mR}{K_f}, \tag{6}$$

$$f_{fric} = \frac{R}{K_f}\bar{f}_{fric}, \tag{7}$$

$$f_{load} = \frac{R}{K_f}\bar{f}_{load}, \tag{8}$$

$$f_{res} = \frac{R}{K_f}\bar{f}_{res}. \tag{9}$$

Thus, we have the following equivalent model:

$$\ddot{x} = \frac{a\dot{x} + u - f_{fric} - f_{load} - f_{res}}{b}. \tag{10}$$

The frictional force affecting the movement of the translator can be modeled as a combination of Coulomb and viscous friction. The mathematical model may be written according to [5] as:

$$f_{fric} = [f_c + f_v|\dot{x}|]sgn(\dot{x}), \tag{11}$$

where f_c is the minimum level of Coulomb friction and f_v is associated with the viscosity constant.

For loading effects which are independent of the direction of motion, f_{load} can be described as:

$$f_{load} = f_l sgn(\dot{x}). \tag{12}$$

Cumulatively, the frictional and load force can be described as one external disturbance F given by:

$$F = [f_1 + f_2|\dot{x}|]sgn(\dot{x}), \tag{13}$$

where $f_1 = f_l + f_{fric}$ and $f_2 = f_v$. Figure 1 graphically illustrates the characteristics of F. Figure 2 is a block diagram depicting the overall model of the servo-mechanical system. It is an objective of this paper to estimate the key characteristics of F using a relay feedback experiment.

Table 1: Parameters of the linear motor

Contents	Units	$LS1-24$
Force Constant (K_f)	N/Amp	10.5
Resistance (R)	Ohms	1.5
Back EMF(K_e)	volt/m/sec	10.5
Length of Travel	m	609.6
Slide Weight	kg	0.59
Armature Inductance(L)	mh	2.2
Peak Forces (F_p)	N	210
Magnetic Attraction	N	730
Peak Current (I_p)	Amps	20.0
Typical Velocity	m/sec	0.5
Maximal Acceleration	m/sec^2	2

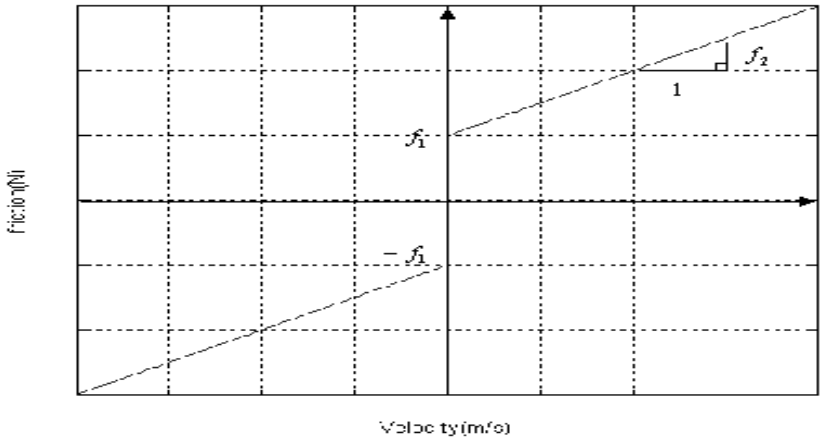

Figure 1: F-$\dot{x}$ characteristics

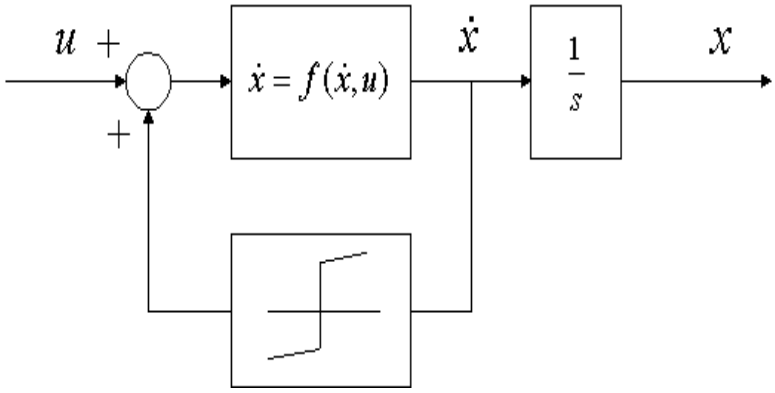

Figure 2: Model of the servo-mechanical system under the influence of friction

3 Proposed Identification Method

Under the dual relay feedback for servo-mechanical system, the closed-loop arrangement depicted in Figure 4 may be posed equivalently as in the configuration of Figure 5, consisting of a parallel relay construct acting on the linear portion of the servo-mechanical system. The second feedback relay ($FR2$ which is cascaded to an integrator) is necessary to excite oscillation at a finite frequency since the phase response of servo-mechanical systems rarely exceeds $-\pi$. Alternatively, the use of an additional deliberate delay element has been reported to achieve similar objective [11], [12].

The parallel relay construct (henceforth called the equivalent relay ER) consists of feedback relays $FR1$ and $FR2$, as well as the inherent system relay SR due to frictional and load forces. The describing function (DF) approximation is thus directly applicable towards the analysis of the feedback system.

The DF of the equivalent relay (N_{ER}) is simply the sum of the individual DFs due to the feedback relays (N_{FR1}), (N_{FR2}) and the inherent system relay (N_{SR}), i.e.

$$N_{ER} = N_{FR1} + N_{FR2} + N_{SR}.$$

According to [13],

$$\begin{aligned} N_{FR1}(a) &= \frac{4h_1}{\pi a}, \\ N_{FR2}(a) &= -j\frac{4h_2}{\pi a}, \\ N_{SR}(a) &= j\left(\frac{4f_1}{\pi a} + f_2\right), \\ N_{ER}(a) &= \frac{4h_1}{\pi a} + j\left(\frac{4(f_1 - h_2)}{\pi a} + f_2\right). \end{aligned}$$

For DF analysis, it is more convenient to work with transfer function of the linear system dynamics. The transfer function of the linear system from u to x can be shown to be

$$G_p(s) = \frac{K_p}{s(T_p s + 1)}, \tag{14}$$

where $K_p = 1/a$ and $T_p = b/a$. Under the relay feedback, the amplitude and oscillating frequency of the limit cycle is thus given approximately by the solution to

$$G_p(j\omega) = -\frac{1}{N_{ER}(a)}, \tag{15}$$

i.e. the intersection of the $G_p(j\omega)$ and the negative inverse DF of the equivalent relay.

The complex equation (15) will generate the following two equations:

$$\begin{aligned} |G_p(j\omega)| &= \left|\frac{1}{N_{ER}(a)}\right|, \\ arg G_p(j\omega) + arg(N_{ER}(a)) &= -\pi. \end{aligned}$$

Clearly, two unknown parameters can be obtained from the solution of these equations.

The negative inverse DF of the equivalent relay is a ray to the origin in the third quadrant of the complex plane, if $h_2 > f_1$ as shown in Figure ?. The angle at which this ray intersects the real axis depends on the relative relay amplitude of h_1 and h_2. In this way, a sustained limit cycle can be induced from servo-mechanical systems, similar to the more conventional single relay setup for industrial processes.

Note that the choice of $h_1 = 0$ and $h_2 > f_1$ will lead to a double integrator phenomenon, where no sustained oscillation can be obtained from relay feedback. When the amplitudes of the feedback relays are chosen to be large compared to that of the inherent relay SR, then the effects of SR become insignificant, i.e.

$$N_{ER} \approx N_{FR1} + N_{FR2}, \tag{16}$$

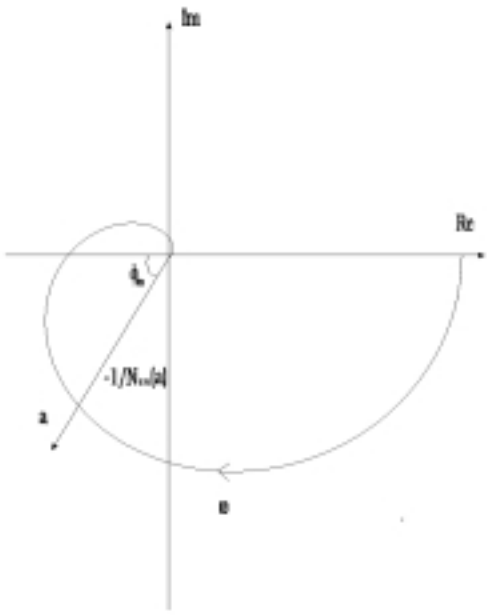

Figure 3: Negative inverse describing function of the modified relay.

and the motor characteristics, K_p and T_p can be derived in the usual manner. By varying h_1 and/or h_2, two relay experiments can be conducted, thus deriving four equations from which all the four unknowns K_p, T_p, f_1 and f_2 can be computed. It is straightforward to show that the parameters can be directly computed from the following equations.

$$\begin{aligned} K_p &= \frac{\pi a_1}{4\sqrt{h_{1,1}^2 + h_{2,1}^2}}\omega_1\sqrt{1+\omega_1^2 T_p^2}, \\ T_p &= \frac{h_{1,1}}{h_{2,1}\omega_1}, \\ f_1 &= \left(-\frac{h_{1,1}a_2}{T_p\omega_1} + \frac{h_{1,2}a_1}{T_p\omega_2} + h_{2,1}a_2 - h_{2,2}a_1\right)/(a_2 - a_1), \\ f_2 &= -\frac{4}{\pi a_1}\left(\frac{h_{1,1}}{T_p\omega_1} + f_1 - h_{2,1}\right). \end{aligned} \tag{17}$$

where ω_1, ω_2 are the sustained oscillating frequencies of the limit cycle oscillations from the relay experiments, a_1 and a_2 are the associated amplitudes of the limit cycles. $h_{1,1}$ and $h_{2,1}$ are the amplitudes used in the first experiment for relay FR1 and FR2 respectively. $h_{1,2}$ and $h_{2,2}$ are the corresponding relay amplitudes used in the second experiment.

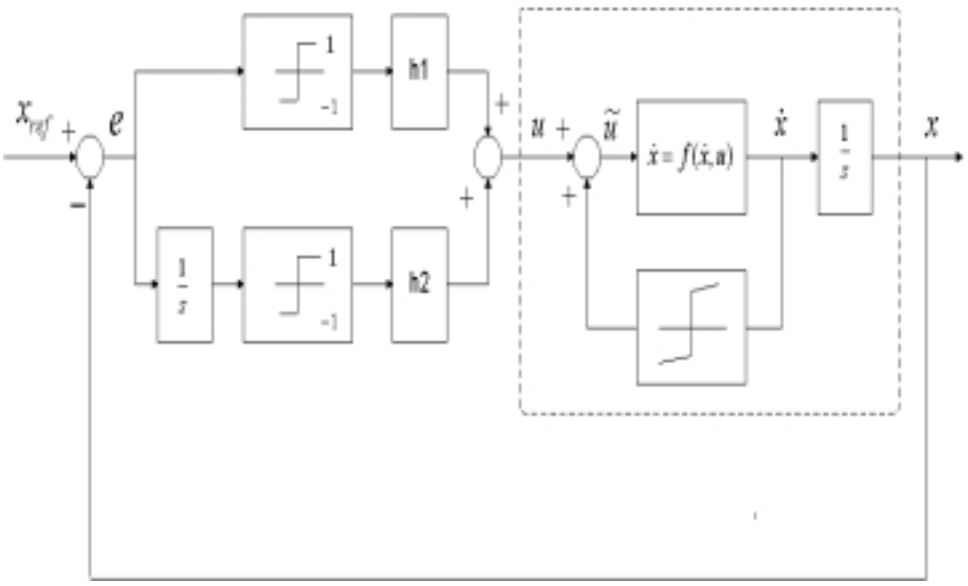

Figure 4: Proposed dual relay setup

4 Simulation

To illustrate the accuracy of the estimates of f_1 and f_2 from the proposed relay method, a simulation example is provided.

Consider the process :

$$G_p(s) = \frac{10}{s(0.2685s + 1)}, \tag{18}$$

with $f_1 = 0.5, f_2 = 0.01$. In the first experiment, we choose $h_1 = 2$ and $h_2 = 1.5$. T_p and K_p are correctly identified as $T_p = 0.265$ and $K_p = 10$ respectively.

In the second experiment, we choose $h_1 = 1$ and $h_2 = 0.7$. f_1 and f_2 are correctly identified as $f_1 = 0.5104$ and $f_2 = 0.0065$. The limit cycle oscillations corresponding to the two experiments are shown in Figure 6 and 7.

5 Adaptive Friction Compensation

Although an initial model of the servo-mechanical system may be obtained according to the aforementioned relay feedback method, the model parameters are usually not precisely known. Furthermore, the system dynamics especially the frictional characteristics can be time varying in nature. This motivates the development of an adaptive control algorithm for the servo-mechanical system.

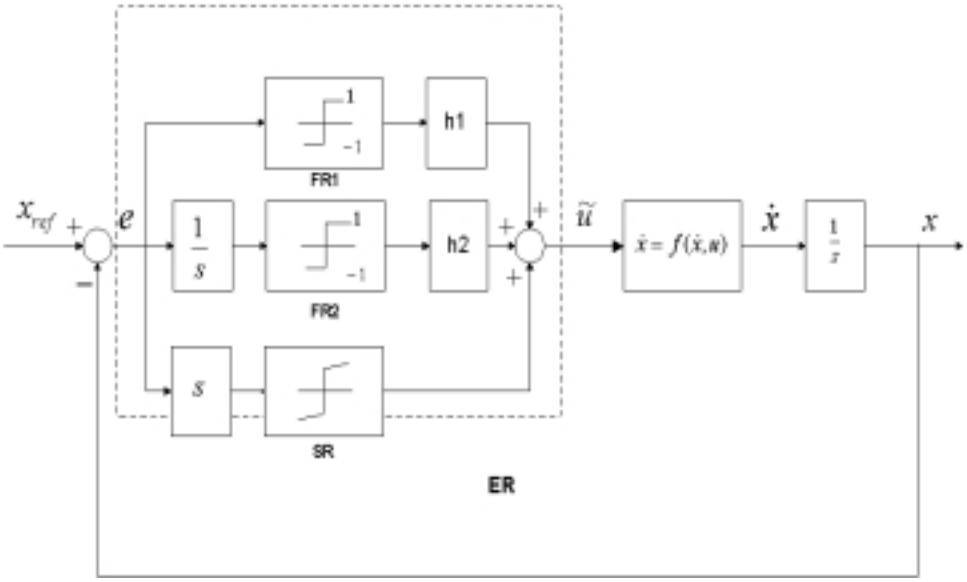

Figure 5: Equivalent system

Define the tracking errors:

$$e(t) = x_d(t) - x(t), \tag{19}$$

$$\dot{e}(t) = \dot{x}_d(t) - \dot{x}(t), \tag{20}$$

where x_d and $\dot{x}_d$ are the desired position and velocity, respectively. To achieve the tracking control, we define a sliding surface [14]:

$$s = \Lambda_1 \int_0^t e(\tau)d\tau + \Lambda_2 e(t) + \dot{e}(t), \tag{21}$$

where Λ_1, Λ_2 are chosen such that the polynomial $\lambda^2 + \Lambda_2\lambda + \Lambda_1$ is Hurwitz.

Here, we define another error metric, $s_\Delta(t)$, as in [14]

$$s_\Delta(t) = s(t) - \delta sat(s(t)/\delta), \tag{22}$$

where $sat(.)$ is a saturation function defined as:

$$sat(x) = \begin{cases} x \;\; if \;\; |x| < 1 \\ sgn(x) \;\; otherwise \end{cases} \tag{23}$$

The function s_Δ has the following useful properties:

(i) if $|s| < \delta$, then $\dot{s}_\Delta = s_\Delta = 0$,

(ii) if$|s| > \delta$, then $\dot{s}_\Delta = \dot{s}$ and $|s_\Delta| = |s| - \delta$,

(iii)$s_\Delta sat(s/\delta) = |s_\Delta|$.

The problem is to design a control law $u(t)$ which ensures that the tracking error metric $s(t)$ lies

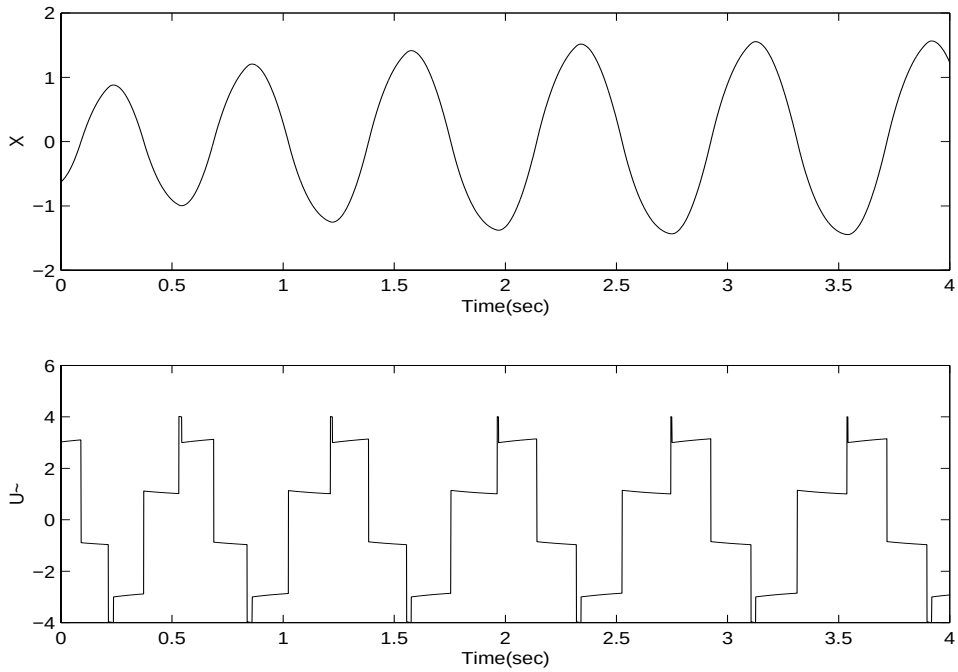

Figure 6: Input/output signals with $h_1 = 2$, $h_2 = 1.5$

in the predetermined boundary δ for all time $t > 0$. The following controller is constructed for the nonlinear system (10).

$$u = -\hat{a}\dot{x} - \hat{b}u_c + \hat{f}_1 sgn(\dot{x}) + \hat{f}_2 sgn(\dot{x})\dot{x} + \hat{f} sgn(s_\Delta), \tag{24}$$

where $\hat{a}$ and $\hat{b}$ are the estimates of a and b respectively; $\hat{f}_1$ represents the estimate of f_1 and $\hat{f}_2$ represents the estimate of f_2; $\hat{f}$ represents an estimate of the bound f on f_{res}, i.e. $|f_{res}| < f$. u_c is an additional control which is given by:

$$u_c = -\Lambda_1 e - \Lambda_2 \dot{e} - \ddot{x}_d - K_v s_\Delta. \tag{25}$$

Differentiating $s(t)$ and using the control (24), the linear motor dynamics (10) may be written in terms of the filtered tracking errors as:

$$\begin{aligned} \dot{s} &+ K_v s_\Delta \\ &= \frac{-\tilde{a}\dot{x} - \tilde{b}u_c + \tilde{f}_1 sgn(\dot{x}) + \tilde{f}_2 sgn(\dot{x})\dot{x} - \hat{f} sgn(s_\Delta) + f}{b}, \end{aligned} \tag{26}$$

where $\tilde{a} = a - \hat{a}, \tilde{b} = b - \hat{b}, \tilde{f}_1 = f_1 - \hat{f}_1, \tilde{f}_2 = f_2 - \hat{f}_2$.

We now specify the parameter update laws:

$$\dot{\hat{a}} = -k_a \dot{x} s_\Delta, \tag{27}$$

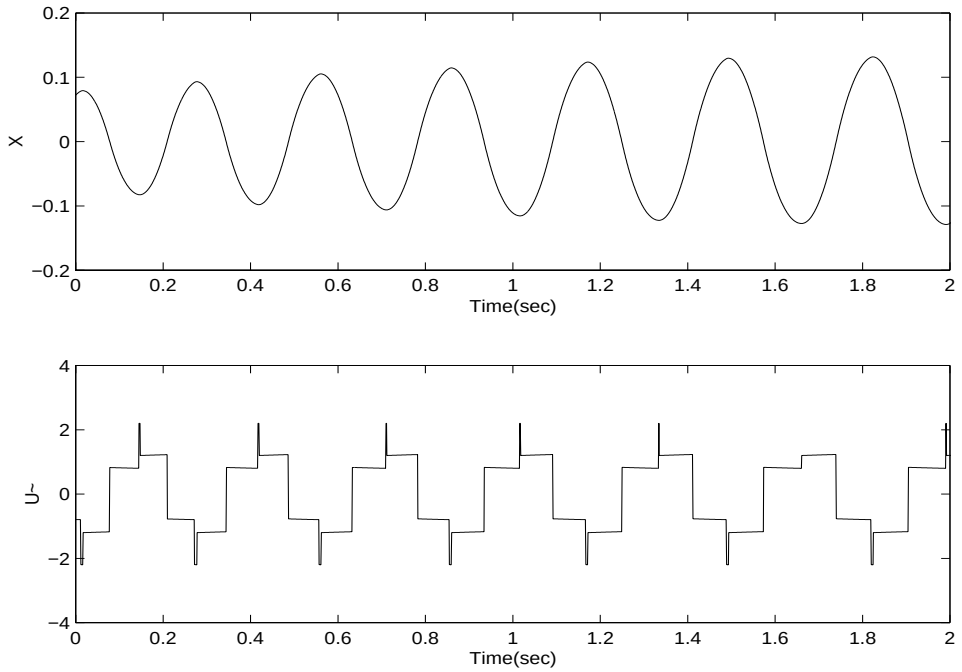

Figure 7: Input/output signals with $h_1 = 1$, $h_2 = 0.7$

$$\dot{\hat{b}} = -k_b u_c s_\Delta, \tag{28}$$

$$\dot{\hat{f}}_1 = k_{f1} sgn(\dot{x}) s_\Delta, \tag{29}$$

$$\dot{\hat{f}}_2 = k_{f2} \dot{x} sgn(\dot{x}) s_\Delta, \tag{30}$$

$$\dot{\hat{f}} = k_f |s_\Delta|. \tag{31}$$

Theorem 1: Convergence of adaptive controller.

Consider the system described by (10) and the control objective of tracking desired trajectories defined by $x_d, \dot{x}_d, \ddot{x}_d$. The control law given by (24) with (27)-(31) ensures that the system states and parameters are uniformly bounded and that $s(t)$ asymptotically converge to the predetermined boundary δ.

Proof:

We first define a Lyapunov function candidate $V(t)$ as

$$V(t) = \frac{1}{2} b s_\Delta^2 + \frac{1}{2k_a} \tilde{a}^2 + \frac{1}{2k_b} \tilde{b}^2 + \frac{1}{2k_{f1}} \tilde{f}_1^2 + \frac{1}{2k_{f2}} \tilde{f}_2^2 + \frac{1}{2k_f} \tilde{f}^2, \tag{32}$$

where $\tilde{f} = f - \hat{f}$. Noting that $\dot{s}_\Delta = \dot{s}$ outside the boundary layer, while $s_\Delta = 0$ inside the boundary

layer, it follows that

$$\begin{aligned}
\dot{V} &= b\dot{s}s_\Delta + \frac{1}{k_a}\tilde{a}\dot{\tilde{a}} + \frac{1}{k_b}\tilde{b}\dot{\tilde{b}} + \frac{1}{k_{f1}}\tilde{f}_1\dot{\tilde{f}}_1 + \frac{1}{k_{f2}}\tilde{f}_2\dot{\tilde{f}}_2 + \frac{1}{k_f}\tilde{f}\dot{\tilde{f}} \\
&= -K_v b s_\Delta^2 - [\tilde{a}\dot{x} + \tilde{b}u_c - \tilde{f}_1 sgn(\dot{x}) - \tilde{f}_2\dot{x}sgn(\dot{x})]s_\Delta \\
&+ [f - \hat{f}sgn(s_\Delta)]s_\Delta \\
&\quad + \frac{1}{k_a}\tilde{a}\dot{\tilde{a}} + \frac{1}{k_b}\tilde{b}\dot{\tilde{b}} + \frac{1}{k_{f1}}\tilde{f}_1\dot{\tilde{f}}_1 + \frac{1}{k_{f2}}\tilde{f}_2\dot{\tilde{f}}_2 + \frac{1}{k_f}\tilde{f}\dot{\tilde{f}} \\
&\leq -K_v b s_\Delta^2 - [\tilde{a}\dot{x} + \tilde{b}u_c - \tilde{f}_1 sgn(\dot{x}) - \tilde{f}_2\dot{x}sgn(\dot{x})]s_\Delta + [f - \hat{f}]|s_\Delta| \\
&\quad + \frac{1}{k_a}\tilde{a}\dot{\tilde{a}} + \frac{1}{k_b}\tilde{b}\dot{\tilde{b}} + \frac{1}{k_{f1}}\tilde{f}_1\dot{\tilde{f}}_1 + \frac{1}{k_{f2}}\tilde{f}_2\dot{\tilde{f}}_2 + \frac{1}{k_f}\tilde{f}\dot{\tilde{f}} \\
&= -K_v b s_\Delta^2 - [\tilde{a}\dot{x} + \tilde{b}u_c - \tilde{f}_1 sgn(\dot{x}) - \tilde{f}_2\dot{x}sgn(\dot{x})]s_\Delta + \tilde{f}|s_\Delta| \\
&\quad - \frac{1}{k_a}\tilde{a}\dot{\hat{a}} - \frac{1}{k_b}\tilde{b}\dot{\hat{b}} - \frac{1}{k_{f1}}\tilde{f}_1\dot{\hat{f}}_1 - \frac{1}{k_{f2}}\tilde{f}_2\dot{\hat{f}}_2 - \frac{1}{k_f}\tilde{f}\dot{\hat{f}}. \qquad (33)
\end{aligned}$$

Substituting the expressions given by (27)-(31) yields

$$\dot{V} \leq -K_v b s_\Delta^2. \qquad (34)$$

Since $b > 0$, it follows that $\dot{V} < 0$. This implies that $s_\Delta, \hat{a}, \hat{b}, \hat{f}_1, \hat{f}_2, \hat{f}$ are uniformly bounded with respect to t. To investigate the convergence of the tracking error, we need to first prove $x, \dot{x}$ are bounded.

Define

$$\sigma_0 = \int_0^t (x_d - x)d\tau. \qquad (35)$$

From (21), we have

$$\begin{bmatrix} \dot{\sigma}_0 \\ \ddot{\sigma}_0 \end{bmatrix} = \begin{bmatrix} 0 & 1 \\ -\Lambda_1 & -\Lambda_2 \end{bmatrix} \begin{bmatrix} \sigma_0 \\ \dot{\sigma}_0 \end{bmatrix} + \begin{bmatrix} 0 \\ 1 \end{bmatrix} s. \qquad (36)$$

Since Λ_1, Λ_2 are chosen such that the polynomial $\lambda^2 + \Lambda_2\lambda + \Lambda_1$ is Hurwitz, the free system of the above equation is asymptotically stable. This together with s_Δ being bounded, implies that $x, \dot{x}$ are bounded.

By definition, $\dot{s}_\Delta(t)$ is either 0 or $\dot{s}(t)$, where $\dot{s}(t)$ is given in (26). Since f is bounded and the system parameters are bounded, this implies that the right side of (26) is bounded. This implies that $\dot{s}$ is bounded. Equation (34) and the positive definiteness of V imply that

$$\lim_{t\to\infty} \int_0^t -\dot{V}(\tau)d\tau = V(0) - \lim_{t\to\infty} V(t) < \infty. \qquad (37)$$

By virtue of Barbalat's lemma, we have

$$\lim_{t\to\infty} \dot{V}(t) = 0, \qquad (38)$$

which, applying (34), further implies

$$\lim_{t\to\infty} s_\Delta = 0. \tag{39}$$

The proof is completed.

Remark 1. Note that $K_v s$ is actually standard PID control. In principle , we can employ the existing PID tuning methods for determining $\Lambda_1, \Lambda_2, K_v$. The initial PID tuning can be based on the relay feedback experiments and subsequent PID refinements based on the adative component.

Remark 2. To achieve high-accuracy tracking, δ should be chosen to be small. However, a small δ may cause control chatter. Therefore, there should be a trade-off between the desired tracking error and the discontinuity of the input tolerable.

Remark 3. It should be noted that while the parameter estimation is self-adapting in the adaptive controller, a good set of initial values provided by the relay experiments is important to ensure good initial transient behaviour and efficient convergence of the parameter estimates. The following simulation example will illustrate this point clearly.

The exact parameters used in the simulation are $a = -10.5$, $b = 0.1429$, $f_1 = 10$ and $f_2 = 10$. The adaptive controller is desired to track a pre-specified trajectory. Figure 8 shows the adaptive control performance with zero initial values, i.e. $a = b = f_1 = f_2 = 0$. The convergence rate is slow and the tracking error is large. Figure 9 shows the performance when initial values of $a = -5$, $b = 0.05$, $f_1 = 6.9979$ and $f_2 = 6.9979$ are used. The tracking error is reduced and convergence rate is faster. Figure 10 shows the performance when good initial values are used with $a = -10$, $b = 0.1$, $f_1 = 9.7971$ and $f_2 = 9.7971$. Both the tracking error and convergence rate are superior compared to the preceeding two cases.

6 Real-Time Experiment

In this section, experimental results are provided to illustrate the effectiveness of the proposed method. Figure 13 shows the experimental setup. The linear motor used is a direct thrust tubular servo motor manufactured by Linear Drives Ltd (LDL)(LD 2504), which has a travel length of 500mm and it is equipped with a Renishaw optical encoder with an effective resolution of $1\mu m$. The dSPACE control development and rapid prototyping system, in particular the DS1102 board, is used. dSPACE integrates the entire development cycle seamlessly into a single environment, so that individual development stages between simulation and test can be run and rerun, without frequent re-adjustment. MATLAB and SIMULINK can be directly used in the development of the final

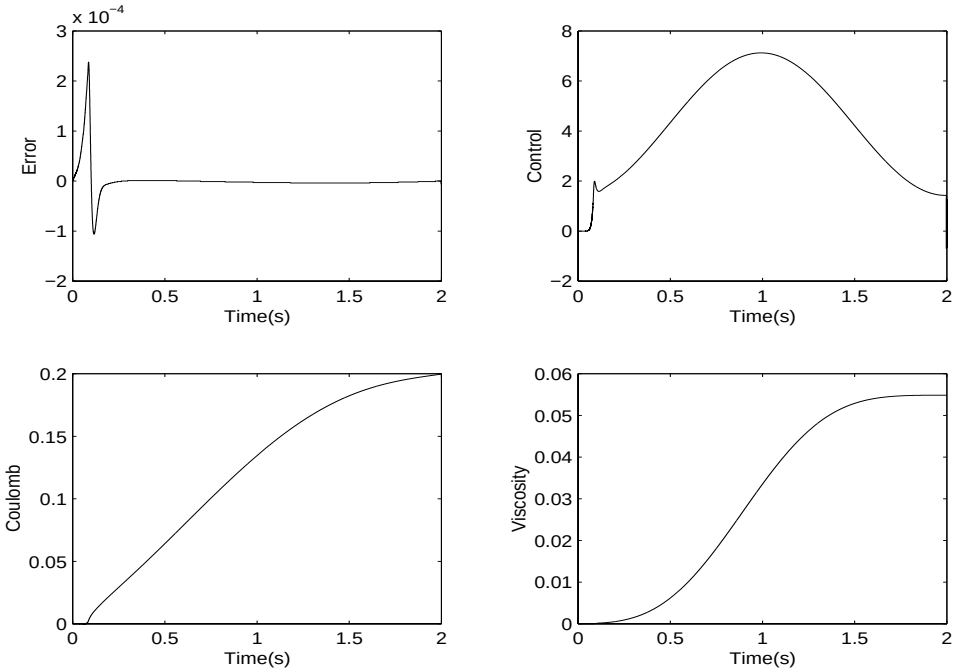

Figure 8: Adaptive control with zero initial values

dSPACE real-time system. The proposed algorithm is written in C and embedded in one S-function block.

Two relay experiments are conducted according to the procedures described in Section 3. The motor parameters are identified as $T_p = 0.073454$ and $K_p = 1.9259 \times 10^5$. The friction parameters are identified as $f_1 = 0.238$ and $f_2 = 0.00062$. The limit cycle oscillations arising from the two experiments are shown in Figure 11 and 12.

With the model parameters, a PID feedback controller can be commissioned and the adaptive feedforward friction compensator can be properly initialised.

Since the mechanical structure and other components in the system have inherent unmodeled high-frequency dynamics which should not be excited, small adaptation factors $k_a, k_b, k_{f1}, k_{f2}, k_f$ should be used for trajectory tracking. The parameters used in the adaptive controller are:

$$K_v = 1200, \Lambda_1 = 600, \Lambda_2 = 1400, k_a = k_b = k_{f1} = k_{f2} = k_f = 10^{-2}, \tag{40}$$

and the desired error tolerance is set to 10.

Figure 14 and 15 shows the tracking performance to a sinusoidal profile with and without the feedforward friction compensator. Clearly, with friction compensator, the root-mean-square (RMS)

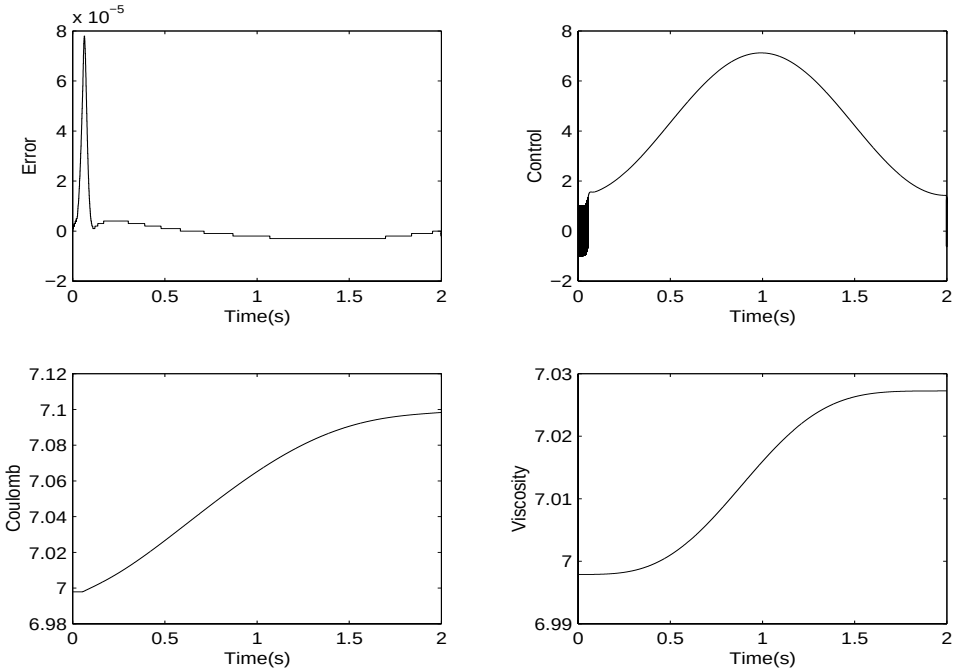

Figure 9: Adaptive control with initial values: $a = -5$, $b = 0.05$, $f_1 = 6.9979$ and $f_2 = 6.9979$

value of the tracking error can be drastically reduced from $11.2\mu m$ to around $1.01\mu m$.

7 Conclusion

A new approach towards modeling of friction in servo-mechanisms using relay feedback has been developed in this paper. The friction model consists of Coulomb and viscous friction components, both of which can be automatically extracted from suitably designed relay experiments. At the same time, the dynamical model of the servo-mechanical system can be obtained from the experiments. In this way, both a PID feedback motion controller and a feedforward friction compensator can be automatically tuned. The friction model obtained is also directly applicable to initialisation of an adaptive control scheme further developed in the paper. Results from simulation and experiments have verified the applicability of the proposed method.

References

[1] Astrom, K.J. and T. Hagglund (1995), *PID Controllers: Theory, Design, and Tuning*, 2nd Edition. Instrument Society of America.

[2] Tan, K.K. T.H.Lee and F.M.Leu (2000), Automatic tuning of 2DOF control for D.C.Servo Motor Systems,*Intelligent automation and soft computing - to appear.*

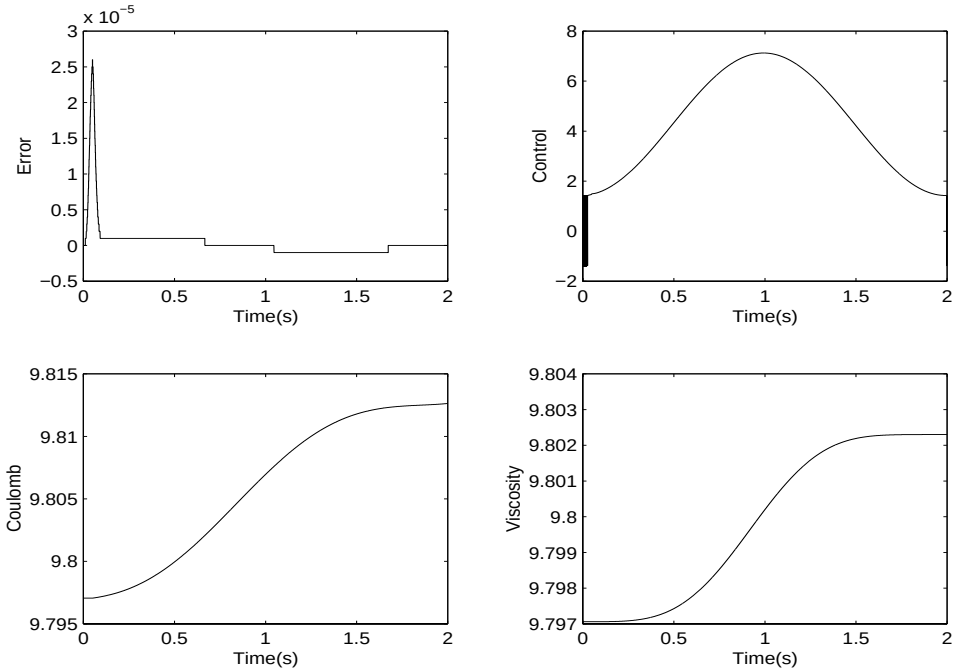

Figure 10: Adaptive control with initial values: $a = -10$, $b = 0.1$, $f_1 = 9.7971$ and $f_2 = 9.7971$

[3] Astrom,K.J and T.Hagglund,C.C.Hang and W.K.Ho (1992), Automatic Tuning and Adaptation for PID controllers-A Survey, *Proceeding of IFAC ACASP'92, France*, pp. 121-126.

[4] Krstic,M., I. Kanellakopoulos and P. Kokotovic (1995). *Nonlinear and Adaptive Control Design*, John Wiley & Sons.

[5] Brian, A. H., D. Pierre and C. D. W. Carlos (1994), A survey of models, analysis tools and compensation methods for the control of machines with friction. *Automatica* **30**(7), pp. 1083–1138.

[6] Armstrong-Helouvry, B., P. Dupont and C.C. de Wit (1994), A survey of models, analysis tools and compensation methods for the control of machines with friction, *Automatica*, **30**(7), pp. 1083-1138.

[7] Taghirad, H.D. and P.R.Bélanger (1998), Robust friction compensator for harmonic drive transmission,*Proc. of 1998 IEEE Int'l Conf. on Control Applications*, pp. 547-551.

[8] Besancon-Voda and G. Besancon (1999), Analysis of a class of two-relay systems, with application to Coulomb friction identification, *Automatica*, **35**(8), pp. 1391-1399.

[9] Fujimoto, Y. and A. Kawamura (1995), Robust servo-system based on two-degree-of-freedom control with sliding mode, *IEEE Trans.on Industrial Electronics*, **42**(3), pp. 272-280.

[10] Anorad Inc. (1999). *Linear servo motors-Anoline Series.* USA.

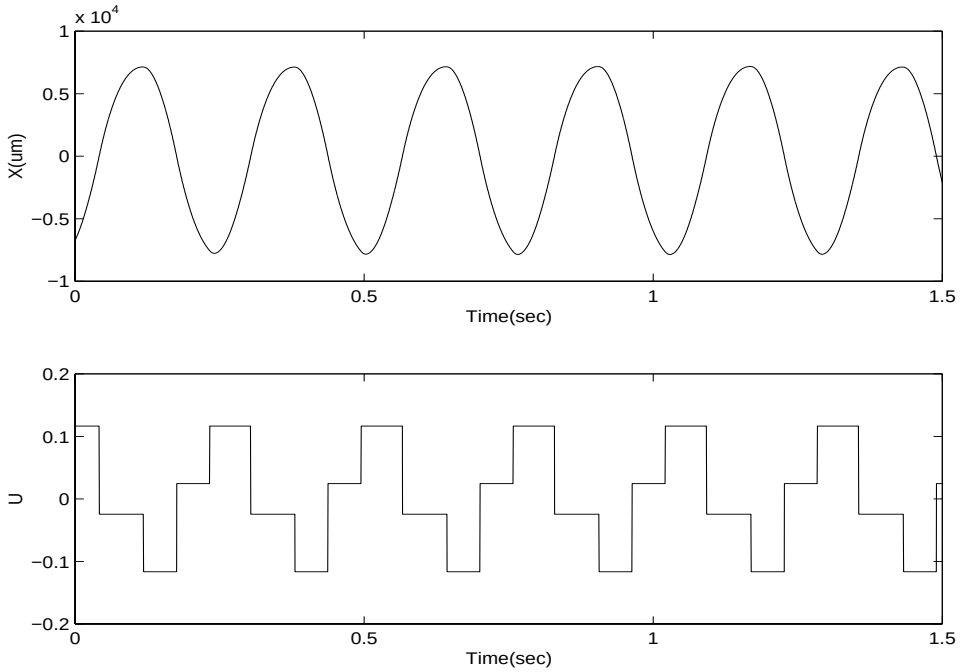

Figure 11: Input-output signals under the first relay experiment

[11] Tan, K.K., H. F. Dou, Y. Q. Chen and T. H. Lee (2000), High precision linear motor control via artificial relay tuning and zero-phase filtering based iterative learning, *IEEE Trans. on Control Systems Technology - to appear.*

[12] Lee, T.H, K.K.Tan, S.Y.Lim, and H.F.Dou (1999), Iterative learning control of permanent magnet linear motor with relay automatic tuning *Mechatronics* 10, pp. 169-190.

[13] Gelb, A. and W.E.V. Velde (1968), *Multiple-input describing functions and nonlinear system design*, McGraw-Hill Book Company: USA.

[14] Slotine, J.J.E. and J.A.Coetsee (1986), Adaptive sliding controller synthesis for non-linear systems, *International Journal of Control*, **43**(6), pp. 1631-1651.

[15] Basak, Amitawa (1996). *Permanent-magnet DC Linear Motors.* Monographs in Electrical and Electronic Engineering. Clarendon Press. Oxford.

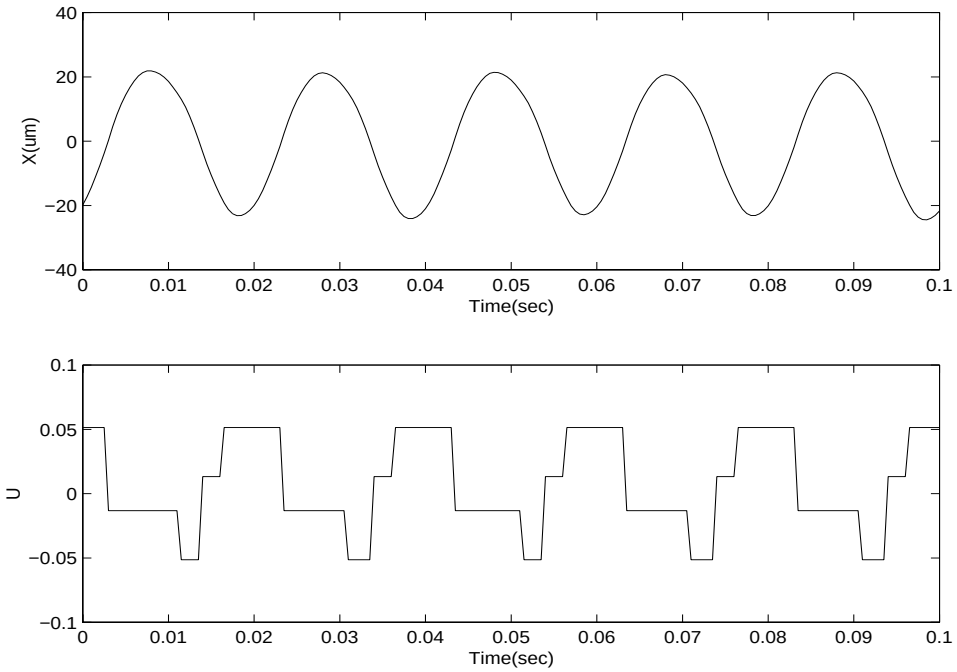

Figure 12: Input-output signals under the second relay experiment

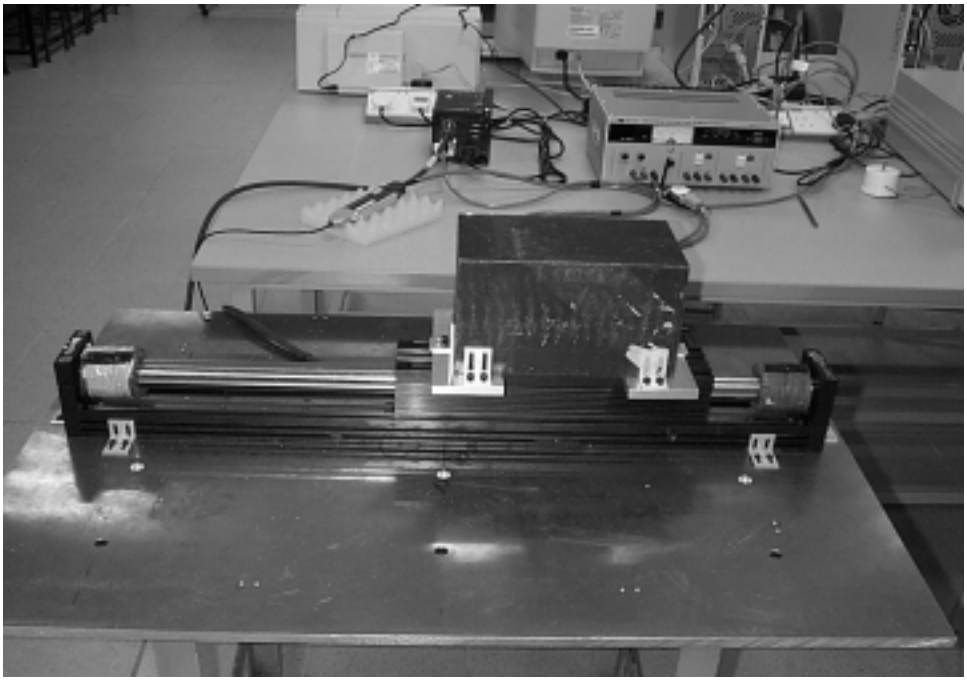

Figure 13: Linear motor used in experiment

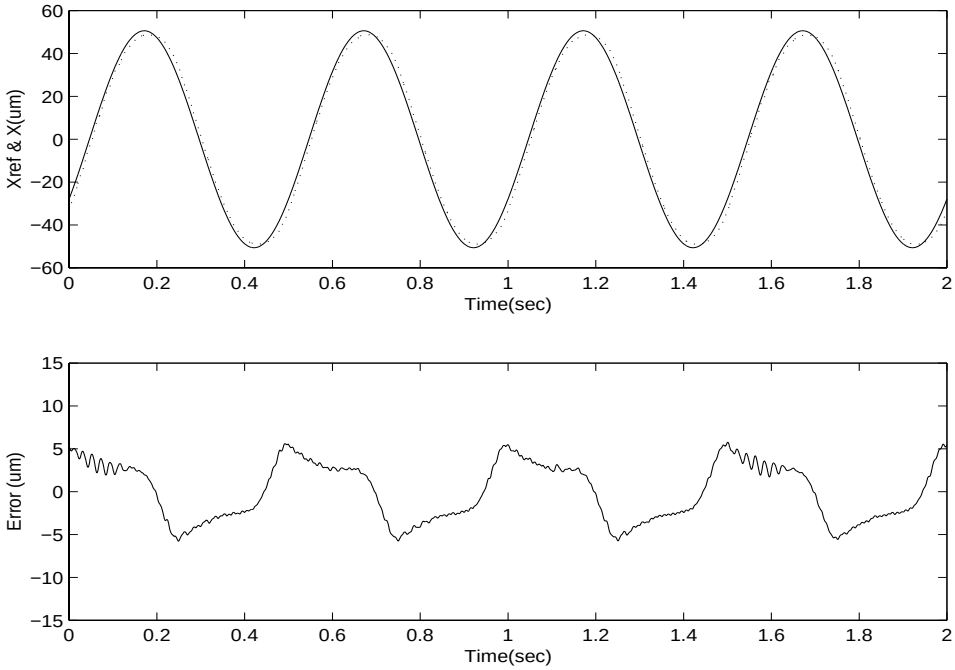

Figure 14: Tracking performance without friction compensation

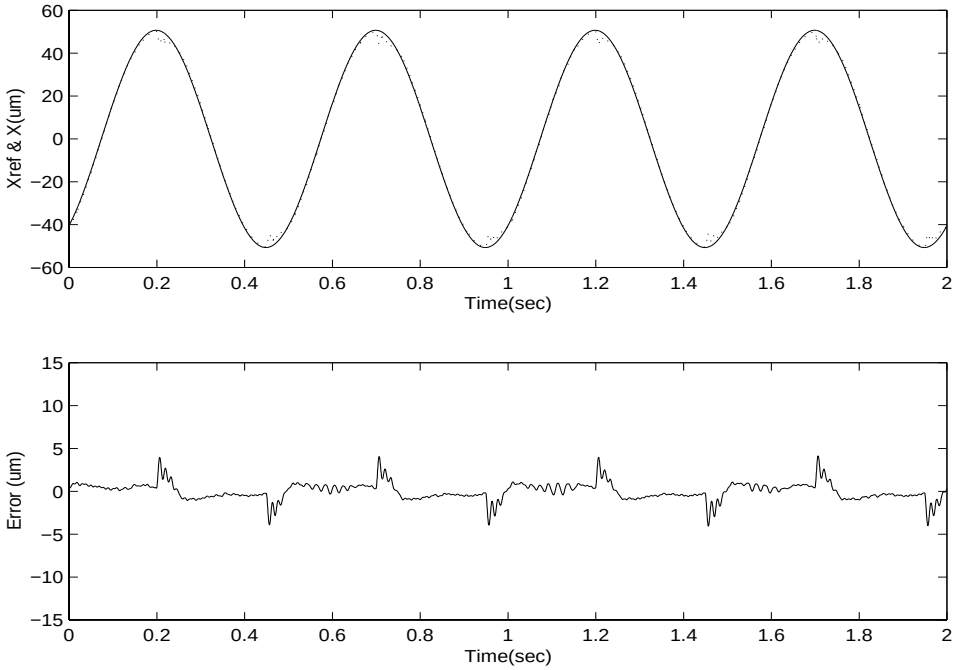

Figure 15: Tracking performance with friction compensation